Singlet Diradical Complexes of Chromium, Molybdenum, and Tungsten with Azo Anion Radical Ligands from M(CO) 6 Precursors

9 AUTHORS, INCLUDING:

Inorganic Chemistry

Article

Singlet Diradical Complexes of Chromium, Molybdenum, and Tungsten with Azo Anion Radical Ligands from $M(CO)_6$ Precursors

Anasuya Sanyal,[†] Sudipta Chatterjee,[†] Alfonso Castiñeiras,[‡] Biprajit Sarkar,[§] Priti Singh,[§] Jan Fiedler,[||] Stanislav Zális,[||] Wolfgang Kaim,*,[§] and Sreebrata Goswami*,[†]

Department of Inorganic Chemistry, Indian Association for the Cultivation of Science, Kolkata 700 032, India, Departamento de Química Inorgánica, Universidade de Santiago de Compostela, 15782 Santiago de Compostela, Spain, Institut für Anorganische Chemie, Universität Stuttgart, Pfaffenwaldring 55, D-70550 Stuttgart, Germany, and J. Heyrovský Institute of Physical Chemistry, v.v.i., Academy of Sciences of the Czech Republic, Dolejškova 3, CZ-18223 Prague, Czech Republic

The homoleptic diamagnetic complexes M(*mer*-L)$_2$, M = Cr, Mo,W (**1a**,**b**, **2a**,**b**, and **4a**,**b**), were obtained by reacting the hexacarbonyls $M(CO)_6$ with the tridentate ligands 2-[(2-*N*-arylamino)phenylazo]pyridine (HL = NH_4C_5N=NC_6H_4N-(H)C_6H_4(H) (HL^a) or NH_4C_5N=NC_6H_4N(H)C_6H_4(CH_3) (HL^b)) in refluxing *n*-octane. In the case of M = Mo, the dinuclear compounds [Mo(L)(pap)]$_2$(μ-O) (**3a**,**b**) (pap = 2-(phenylazo)pyridine), were obtained as second products in moist solvent. X-ray diffraction analysis for Cr(L^b)$_2$ (**1b**), Mo(L^a)$_2$ (**2a**), and W(L^a)$_2$ (**4a**) reveals considerably distorted-octahedral structures with trans-positioned azo-N atoms and cis-positioned 2-pyridyl-N and anilido nitrogen atoms. Whereas the N_{azo}–M–N_{azo} angle is larger than 170°, the other two trans angles are smaller, at about 155° (M = Cr, **1b**) or 146° (M = Mo, W; **2a**, **4a**), due to the overarching bite of the mer-tridentate ligands. The bonds from M to the neutral 2-pyridyl-N atoms are distinctly longer by more than 0.08 Å than those to the anilido or azo nitrogen atoms, reflecting negative charge on the latter. The N–N bond distances vary between 1.339(2) Å for **1b** and 1.373(3) Å for **4a**, clearly indicating the azo radical anion oxidation state. Considering the additional negative charge on anilido-N, the mononuclear complexes are thus formulated as $M^{IV}(L^{•2-})_2$. The diamagnetism of the complexes as shown by magnetic susceptibility and ^{1}H NMR experiments is believed to result from spin–spin coupling between the trans-positioned azo radical functions, resulting in a singlet diradical situation. The experimental structures are well reproduced by density functional theory calculations, which also support the overall electronic structure indicated. The dinuclear **3a** with N–N distances of 1.348(10) Å for L^a and 1.340(9) Å for pap is also formulated as an azo anion radical-containing molybdenum(IV) species, i.e., [Mo^{IV}(L$^{•2-}$)(pap$^{•-}$)]$_2$(μ-O). All compounds can be reversibly reduced; the Cr complexes **1a**,**b** are also reversibly oxidized in two steps. Electron paramagnetic resonance spectroscopy indicates metal-centered spin for **1a**$^+$ and **1a**$^-$ and $g \approx 2$ signals for **2a**$^-$, **3a**$^+$, **3a**$^-$, and **4a**$^-$. Spectroelectrochemistry in the UV–vis–NIR region showed small changes for the reduction of **2a**, **3a**, and **4a** but extensive spectral changes for the reduction and oxidation of **1a**.

Introduction

Transition-metal complexes with coordinated organic radicals[1–5] have attracted considerable attention during the recent years, primarily caused by the realization that such species are active[6] in biological redox processes. To under- stand their reactivities and functions, a clear understanding of the bonding and of the physical characteristics is essential. Consequently, a large variety of transition-metal-stabilized organic radical complexes has been synthesized in the recent years and subjected to detailed investigations.

In this paper, we report our study on the synthesis and characterization of a family of stable azo anion radical

* To whom correspondence should be addressed. E-mail: icsg@iacs.res.in (S.G.), Kaim@iac.uni-stuttgart.de (W.K.).
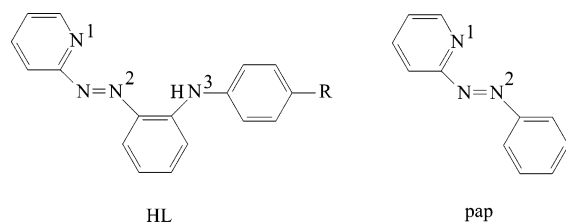† Indian Association for the Cultivation of Science.
‡ Universidade de Santiago de Compostela.
§ Universität Stuttgart.
|| Academy of Sciences of the Czech Republic.

(1) (a) Kaim, W. *Coord. Chem. Rev.* **1987**, *76*, 187. (b) Pierpont, C. G.; Lange, C., W. *Prog. Inorg. Chem.* **1994**, *41*, 331. (c) Chaudhuri, P.; Wieghardt, K. *Prog. Inorg. Chem.* **2001**, *50*, 151.

Chart 1

HL   pap

R = H   : HL^a

R = CH$_3$: HL^b

complex	numbering	complex	numbering
Cr(L^a)$_2$	**1a**	Cr(L^b)$_2$	**1b**
Mo(L^a)$_2$	**2a**	Mo(L^b)$_2$	**2b**
[(L^a)(pap)Mo]$_2$O	**3a**	[(L^b)(pap)Mo]$_2$O	**3b**
W(L^a)$_2$	**4a**	W(L^b)$_2$	**4b**

complexes,[5,7,8] M(L)$_2$, coordinated to group VI metal ions. The coordination chemistry of the tridentate azo aromatic ligand (HL, Chart 1) has been investigated in our laboratory.[9] Several interesting examples including low-spin complexes[9b,c] of Fe^II and Fe^III have been reported. It may be relevant to add here that there has been renewed interest in the coordination chemistry of tridentate nitrogen donors[10] following the discovery that these complexes actively catalyze[11] olefin polymerization. The azo aromatic ligands in these complexes are known to undergo facile reduction, generating azo anion radicals in solution, but such radicals have

generally eluded[12] isolation. In the course of our studies in these systems, we have recently isolated[13] a series of molybdenum(IV)-stabilized diradical complexes, Mo(L)$_2$. Their synthesis was achieved from ammonium heptamolybdate using triphenylphosphine as the reducing agent. We proposed that PPh$_3$ mediates the reductive oxo transfer in the said reaction, yielding low-valent Mo^II(L^−)$_2$ intermediates, which then underwent internal electron transfer to produce stable tetravalent molybdenum complexes of the dianionic radical ligand [L^•2−]. However, similar reactions of the polyoxometalates of Cr and W failed to produce any isolable products.

In search of a general synthetic procedure for such systems, we have now discovered that their synthesis can be successfully achieved from the metal hexacarbonyls, M(CO)$_6$ (M= Cr, Mo, W). While selecting metal hexacarbonyls as the starting compounds, it was anticipated that the azo aromatic ligand [L]^− would substitute CO ligands completely as it happened[14] in the reactions of M(CO)$_6$ with 2-(phenylazo)-pyridine. Bond−structure parameters, spectroscopic data, and density functional theory (DFT) calculations point to a predominant azo anion radical description of the ligands in the species that are presented in this work.

(2) (a) Pierpont, C. G. *Coord. Chem. Rev.* **2001**, *219−221*, 415. (b) Pierpont, C. G. *Coord. Chem. Rev.* **2001**, *216-217*, 95. (c) Rajca, A. *Chem. Rev.* **1994**, *94*, 871. (d) Buchanan, R. M.; Downs, H. H.; Shorthill, W. B.; Pierpont, C. G.; Kessel, S. L.; Hendrickson, D. N. *J. Am. Chem. Soc.* **1978**, *100*, 4318. (e) Ziegler, M.; Davis, A. V.; Johnson, D. W.; Raymond, K. N. *Angew. Chem., Int. Ed.* **2003**, *42*, 665. (f) Duhme, A.-K.; Dauter, Z.; Hider, R. C.; Pohl, S. *Inorg. Chem.* **1996**, *35*, 3059. (g) Duhme, A.-K.; Davies, S. C.; Hughes, D. L. *Inorg. Chem.* **1998**, *37*, 5380. (h) Ohtsu, H.; Tanaka, K. *Angew. Chem., Int. Ed.* **2004**, *43*, 6301. (i) Shimazaki, Y.; Tani, F.; Fukui, K.; Naruta, Y.; Yamauchi, O. *J. Am. Chem. Soc.* **2003**, *125*, 10512. (j) Suenaga, Y.; Pierpont, C. G. *Inorg. Chem.* **2005**, *44*, 6183. (k) Bhattacharya, S.; Gupta, P.; Basuli, F.; Pierpont, C. G. *Inorg. Chem.* **2002**, *41*, 5810. (l) Shaikh, N.; Goswami, S.; Panja, A.; Wang, X.-Y.; Gao, S.; Butcher, R. J.; Banerjee, P. *Inorg. Chem.* **2004**, *43*, 5908.

(3) (a) Sawyer, D. T.; Srivatsa, G. S.; Bodini, M. E.; Schaefer, W. P.; Wing, R. M. *J. Am. Chem. Soc.* **1986**, *108*, 936. (b) Ray, K.; Weyhermüller, T.; Goossens, A.; Craje, M. W. J.; Wieghardt, K. *Inorg. Chem.* **2003**, *42*, 4082. (c) Sellmann, D.; Binder, H.; Häusinger, D.; Heinemann, F. W.; Sutter, J. *Inorg. Chim. Acta* **2000**, *300−302*, 829.

(4) (a) Verani, C. N.; Gallert, S.; Bill, E.; Weyhermüller, T.; Wieghardt, K.; Chaudhuri, P. *Chem. Commun.* **1999**, 1747. (b) Chaudhuri, P.; Verani, C. N.; Bill, E.; Bothe, E.; Weyhermüller, T.; Wieghardt, K. *J. Am. Chem. Soc.* **2001**, *123*, 2213. (c) Chun, H.; Verani, C. N.; Chaudhuri, P.; Bothe, E.; Bill, E.; Weyhermüller, T.; Wieghardt, K. *Inorg. Chem.* **2001**, *40*, 4157. (d) Chun, H.; Weyhermüller, T.; Bill, E.; Wieghardt, K. *Angew. Chem., Int. Ed.* **2001**, *40*, 2489. (e) Noveron, J. C.; Olmstead, M. M.; Mascharak, P. K. *Inorg. Chem.* **1998**, *37*, 1138. (f) Liaw, W.-F.; Lee, N.-H.; Chen, C.-H.; Lee, C.-M.; Lee, G.-H.; Peng, S.-M. *J. Am. Chem. Soc.* **2000**, *122*, 488.

(5) (a) Doslik, N.; Sixt, T.; Kaim, W. *Angew. Chem.* **1998**, *110*, 2125; *Angew. Chem., Int. Ed.* **1998**, *37*, 2403. (b) Kaim, W.; Kohlmann, S. *Inorg. Chem.* **1990**, *29*, 1898. (c) Kaim, W.; Kohlmann, S.; Ernst, S.; Olbrich-Deussner, B.; Bessenbacher, C.; Schulz, A. *J. Organomet. Chem.* **1987**, *321*, 215. (d) Kaim, W. *Coord. Chem. Rev.* **2001**, *219−221*, 463. (e) Kaim, W. *Coord. Chem. Rev.* **2002**, *230*, 127.

(6) (a) Jadzewski, B. A.; Tolman, W. B. *Coord. Chem. Rev.* **2000**, *200−202*, 633. (b) Stubbe, J.; Van der Donk, W. A. *Chem. Rev.* **1998**, *98*, 705. (c) Kaim, W. *Dalton Trans.* **2003**, 761.

(7) (a) Shivakumar, M.; Pramanik, K.; Ghosh, P.; Chakravorty, A. *Inorg. Chem.* **1998**, *37*, 5968. (b) Banerjee, S.; Bhattacharyya, S.; Dirghangi, B. K.; Menon, M.; Chakravorty, A. *Inorg. Chem.* **2000**, *39*, 6. (c) Pramanik, K.; Shivakumar, M.; Ghosh, P.; Chakravorty, A. *Inorg. Chem.* **2000**, *39*, 195. (d) Shivakumar, M.; Pramanik, K.; Bhattacharyya, I.; Chakravorty, A. *Inorg. Chem.* **2000**, *39*, 4332.

(8) (a) Sarkar, B.; Patra, S.; Fiedler, J.; Sunoj, R. B.; Janardanan, D.; Mobin, S. M.; Niemeyer, M.; Lahiri, G. K.; Kaim, W. *Angew. Chem., Int. Ed.* **2005**, *44*, 5655. (b) Schwach, M.; Hausen, H.-D.; Kaim, W. *Inorg. Chem.* **1999**, *38*, 2242.

(9) (a) Saha, A.; Ghosh, A. K.; Majumder, P.; Mitra, K. N.; Mondal, S.; Rajak, K. K.; Falvello, L. R.; Goswami, S. *Organometallics* **1999**, *18*, 3772. (b) Saha, A.; Majumder, P.; Goswami, S. *J. Chem. Soc., Dalton Trans.* **2000**, 1703. (c) Saha, A.; Majumder, P.; Peng, S.-M.; Goswami, S. *Eur. J. Inorg. Chem.* **2000**, 2631. (d) Kamar, K. K.; Saha, A.; Castiñeiras, A.; Hung, C.-H.; Goswami, S. *Inorg. Chem.* **2002**, *41*, 4531.

(10) Bruin, B. D.; Bill, E.; Bothe, E.; Weyhermüller, T.; Wieghardt, K. *Inorg. Chem.* **2000**, *39*, 2936.

(11) (a) Brintzinger, H. H.; Fischer, D.; Muelhaupt, R.; Rieger, B.; Waymouth, R. M. *Angew. Chem., Int. Ed. Engl.* **1995**, *34*, 1143. (b) Bockman, M. *J. Chem. Soc., Dalton Trans.* **1996**, 255. (c) Coates, G. W.; Waymouth, R. M. In C*omprehensive Organometallic Chemistry II*; Abel, E. W., Stone, F. G. A., Wilkinson, G., Hegedus, L., Eds.; Pergamon Press: Oxford, U.K., 1995; Vol. 12, p 1193. (c) Johnson, L. K.; Killian, C. M.; Brookhart, M. S. *J. Am. Chem. Soc.* **1995**, *117*, 6414. (d) Killian, C. M.; Tempel, D. J.; Johnson, L. K.; Brookhart, M. S. *J. Am. Chem. Soc.* **1996**, *118*, 11664. (e) Britovsek, G. J. P.; Gibson, V. C.; Kimberley, B. S.; Maddox, P. J.; McTavish, S. J.; Solan, G. A.; White, A. J. P.; Williams, D. J. *Chem. Commun.* **1998**, 849. (f) Small, B. L.; Brookhart, M.; Bennett, A. M. A. *J. Am. Chem. Soc.* **1998**, *120*, 4049. (g) Britovsek, G. J. P.; Gibson, V. C.; Wass, D. F. *Angew. Chem., Int. Ed.* **1999**, *38*, 428.

(12) (a) Sadler, J. L.; Bard, A. J. *J. Am. Chem. Soc.* **1968**, *90*, 1979. (b) Jonson, C. J.; Chang, R. *J. Chem. Phys.* **1965**, *43*, 3183.

(13) Sanyal, A.; Banerjee, P.; Lee, G.-H.; Peng, S.-M.; Hung, C.-H.; Goswami, S. *Inorg. Chem.* **2004**, *43*, 7456.

(14) Ackermann, M. N.; Barton, C. R.; Deodene, C. J.; Specht, E. M.; Keill, S. C.; Schreiber, W. E.; Kim, H. *Inorg. Chem.* **1989**, *28*, 397.

Experimental Section

Materials. The metal carbonyls $M(CO)_6$ (M = Cr, Mo, W) were Aldrich reagents, and *n*-octane was obtained from Spectrochem India. The ligands HL^a and HL^b were prepared by following the reported[9] procedure. Tetraethylammoniumperchlorate was prepared and recrystallized as reported earlier. ***Caution: Perchlorates have to be handled with care and appropriate safety precautions.*** Purissgrade dry *n*-octane solvent was obtained from Fluka. All other chemicals and solvents were of reagent grade and used as received.

Instrumentation. Electron paramagnetic resonance (EPR) spectra in the X band were recorded with a Bruker System EMX. ^1H NMR spectra were taken on a Bruker Avance DPX 300 spectrometer, and $SiMe_4$ was used as the internal standard. The infrared spectra were obtained using a Perkin-Elmer 783 spectrophotometer. UV–vis–NIR absorption spectra were recorded on a J&M TIDAS spectrophotometer. Electrochemical measurements were performed at 298 K under a dry nitrogen atmosphere on a PC-controlled PAR model 273A electrochemistry system. A platinum disk (working) electrode, a platinum wire (auxiliary) electrode, and an aqueous saturated calomel reference electrode (SCE) were used in a three-electrode configuration. The $E_{1/2}$ value for the ferrocenium–ferrocene couple under our experimental condition was 0.39 V. A Perkin-Elmer 240C elemental analyzer was used to collect microanalytical data (C, H, N). Electrospray ionization (ESI) mass spectra were recorded on a Micromass Q-TOF mass spectrometer (serial No. YA 263). A two-electrode capillary was used in radical complex generation for X-band EPR studies. Spectroelectrochemistry was performed with an optically transparent thin-layer electrolysis cell.

Syntheses. The complexes were generally synthesized by reacting the metal carbonyls $M(CO)_6$ (M = Cr, Mo, W) with the corresponding ligands in refluxing commercially available *n*-octane. The complexes of the general formula ML_2 were obtained as the major products. However, in the case of molybdenum, a dinuclear compound $[Mo(L)(pap)]_2O$ (pap = 2-(phenylazo)pyridine) was obtained as minor product.

Synthesis of $Cr(L)_2$. $Cr(L^a)_2$ (1a). A mixture of 40 mg (0.18 mmol) of $Cr(CO)_6$ and 100 mg (0.365 mmol) of HL^a in 30 mL of *n*-octane was heated at reflux for 4 h. During this period, the color of the solution changed from red to brown. The crude dark mass, obtained by the evaporation of the solvent, was dissolved in the minimum amount of dichloromethane and loaded on a preparative silica gel thin-layer chromatography (TLC) plate for purification. Toluene was used as the eluent. A brown zone that moved ahead of the unreacted red ligand band was collected, and the solvent was evaporated. The residue was crystallized by the slow diffusion of a dichloromethane solution of the compound into hexane. Yield: 75%. FT-IR (KBr, cm^{-1}): 1590, 1618 [$\nu(C=C) + \nu(C=N)$], 1247, 1265 [$\nu(N=N)$]. ESI-MS, *m/z*: 599 [MH]$^+$. Anal. Calcd for $C_{34}H_{26}N_8Cr$: C, 68.23; H, 4.35; N, 18.73. Found: C, 68.25; H, 4.14; N, 18.73.

The compound $Cr(L^b)_2$ (**1b**) was synthesized similarly using the ligand HL^b in place of HL^a. Yield: 73%. FT-IR (KBr, cm^{-1}): 1590, 1601 [$\nu(C=C) + \nu(C=N)$], 1247, 1267 [$\nu(N=N)$]. ESI-MS, *m/z*: 627 [MH]$^+$. Anal. Calcd for $C_{36}H_{30}N_8Cr$: C, 69.01; H, 4.79; N, 17.89. Found: C, 69.08; H, 4.77; N, 17.88.

Synthesis of $W(L)_2$. The compounds **4a,b** were synthesized following a similar procedure as above by reacting appropriate quantities of $W(CO)_6$ and HL. However, the reactions in these cases are sluggish, and the bischelated complexes $W(L)_2$ were obtained in ca. 45% yield after 120 h of reflux.

$W(L^a)_2$ (4a). Yield: 45%. FT-IR (KBr, cm^{-1}): 1590, 1618 [ν-(C=C) + ν(C=N)], 1240, 1250 [$\nu(N=N)$]. ESI-MS, *m/z*: 731

[MH]$^+$. Anal. Calcd for $C_{34}H_{26}N_8W$: C, 55.89; H, 3.56; N, 15.34. Found: C, 55.93; H, 3.51; N, 15.32.

$W(L^b)_2$ (4b). Yield: 46%. FT-IR (KBr, cm^{-1}): 1595, 1618 [ν-(C=C) + ν(C=N)], 1240, 1255 [$\nu(N=N)$]. ESI-MS, *m/z*: 759 [MH]$^+$. Anal. Calcd for $C_{36}H_{30}N_8W$: C, 56.99; H, 3.96; N, 14.77. Found: C, 56.92; H, 3.94; N, 14.76.

Synthesis of Mo Complexes: $Mo(L)_2$ and $[Mo(L)(pap)]_2O$. The reactions of $Mo(CO)_6$ and HL were similarly performed as noted above. In this case, the reaction time was 2 h. The major products MoL_2 (**2a, 2b**) were obtained from a TLC plate using toluene as the eluent. A second reddish-brown zone (($Mo(L)$-(pap))$_2O$, (**3a, 3b**)) was eluted with a 20:1 dichloromethane–acetonitrile solution mixture and was finally crystallized by the slow diffusion of a dichloromethane solution of the compound into acetonitrile. However, if the reaction is performed with dry *n*-octane (Fluka, puriss grade) maintaining a dry condition, formation of the dimetallic compounds **3a** and **3b** can be avoided.

$Mo(L^a)_2$ (2a). Yield: 65%. FT-IR (KBr, cm^{-1}): 1595, 1610 [ν-(C=C) + ν(C=N)], 1250, 1280 [$\nu(N=N)$]. ESI-MS, *m/z*: 643 [MH]$^+$. Anal. Calcd for $C_{34}H_{26}N_8Mo$: C, 63.56; H, 4.05; N, 17.45. Found: C, 63.48; H, 4.01; N, 17.50.

$Mo(L^b)_2$ (2b). Yield: 63%. FT-IR (KBr, cm^{-1}): 1575, 1610 [ν-(C=C) + ν(C=N)], 1235, 1280 [$\nu(N=N)$]. ESI-MS, *m/z*: 672 [MH]$^+$. Anal. Calcd for $C_{36}H_{30}N_8Mo$: C, 64.48; H, 4.48; N, 16.72. Found: C, 64.42; H, 4.41; N, 16.65.

$[Mo(L^a)(pap)]_2O$ (3a). Yield: 5%. FT-IR (KBr, cm^{-1}): 1585, 1610 [ν(C=C) + ν(C=N)], 1260, 1275 [$\nu(N=N)$]. ESI-MS, *m/z*: 1121 [MH]$^+$. Anal. Calcd for $C_{56}H_{44}N_{14}OMo_2$: C, 60.00; H, 3.93; N, 17.50. Found: C, 59.92; H, 3.95; N, 17.52.

$[Mo(L^b)(pap)]_2O$ (3b). Yield: 5%. FT-IR (KBr, cm^{-1}): 1585, 1600 [ν(C=C) + ν(C=N)], 1255, 1265 [$\nu(N=N)$]. ESI-MS, *m/z*: 1149 [MH]$^+$. Anal. Calcd for $C_{58}H_{48}N_{14}OMo_2$: C, 60.63; H, 4.18; N, 17.07. Found: C, 60.49; H, 4.11; N, 17.05.

X-ray Structure Determination. Crystallographic data for the compounds **1b**, **3a**, and **4a** are collected in Table 1. Suitable X-ray quality crystals were obtained by the slow diffusion of dichloromethane solutions of compounds **1b** and **3a** into hexane and

Table 1. Crystallographic Data of **1b**, **3a**, and **4a**

	1b	3a	4a
empirical formula	$C_{36}H_{30}N_8Cr$	$C_{56}H_{44}N_{14}OMo_2$	$C_{34}H_{26}N_8W$
molecular mass	626.68	1120.93	730.48
T (K)	293(2)	293(2)	293(2)
cryst syst	orthorhombic	monoclinic	triclinic
space group	*Pbca*	*P2$_1$/c*	*P$\bar{1}$*
a (Å)	17.069(2)	12.887(14)	10.4134(14)
b (Å)	18.518(2)	13.048(14)	17.031(2)
c (Å)	19.202(3)	30.18(3)	16.337(2)
α (deg)	90	90	90.058(2)
β (deg)	90	93.941(19)	104.629(2)
γ (deg)	90	90	89.990(2)
V (Å^3)	6069.44(14)	5063(9)	2803.4(7)
Z	8	4	4
D_{calcd} (mg/m^3)	1.372	1.471	1.731
cryst dimens (mm^3)	$0.37 \times 0.17 \times 0.14$	$0.24 \times 0.16 \times 0.13$	$0.2 \times 0.1 \times 0.1$
θ range for data collection (deg)	2.39–28.3	1.35–25.26	2.02–28.3
GOF	1.322	1.027	1.047
wavelength (Å)	0.71073	0.71073	0.71073
reflns collected	38 681	51 338	18 772
unique reflns	7524	8891	13 278
largest diff between peak and hole (e Å^{-3})	0.782, −0.575	0.709, −1.279	1.583, −0.883
final *R* indices [$I > 2\sigma(I)$]	R1 = 0.0585	R1 = 0.0607	R1 = 0.0258
	wR2 = 0.1228	wR2 = 0.1212	wR2 = 0.0675

acetonitrile, respectively, while crystals of **4a** were obtained by the slow evaporation of a chloroform−hexane solution of the compound.

All data were collected on a Bruker SMART APEX diffractometer, equipped with graphite monochromated Mo Kα radiation ($\lambda = 0.71073$ Å), and were corrected for Lorentz-polarization effects. **1b**: A total of 38 681 reflections were collected, out of which 7524 were unique ($R_{\text{int}} = 0.059$), satisfying the ($I > 2\sigma(I)$) criterion, and were used in subsequent analysis. **3a**: A total of 51 338 reflections were collected, out of which 8891 were unique ($R_{\text{int}} = 0.0573$), satisfying the ($I > 2\sigma(I)$) criterion, and were used in subsequent analysis. **4a**: A total of 18 772 reflections were collected, out of which 13 278 were unique ($R_{\text{int}} = 0.017$), satisfying the ($I > 2\sigma(I)$) criterion, and were used in subsequent analysis.

The structures were solved by employing the *SHELXS-97*[15] program package and refined by full-matrix least-squares based on F^2 (*SHELXL-97*).[16] All hydrogen atoms were added in calculated positions.

DFT Calculations. The electronic structure calculations on complexes ML$_2$ have been done by DFT methods using the *Gaussian 03*[17] and Amsterdam Density Functional (*ADF2005.01*[18]) program packages.

Either the hybrid Becke's three parameter functional with the Lee, Yang, and Parr correlation functional (B3LYP)[19] (G98/B3LYP) or the hybrid functional of Perdew, Burke, and Ernzerhof[20] (PBE0) were used within *Gaussian* (G03/B3LYP) together with 6-31G* polarized double-ζ basis sets[21] for C, N, H, and Cr atoms and effective-core pseudopotentials and corresponding optimized sets of basis functions for Mo and W atoms.[22]

Within the ADF program, Slater-type orbital basis sets of triple-ζ quality with two polarization functions for Cr, Mo, and W atoms and with one polarization function for C, N, and O atoms were employed. Inner shells were represented by the frozen-core approximation (conditions of 1s for C, N, and O, 1s-3p for Cr, 1s-3p for Mo, and 1s-4d for W were kept frozen). Core electrons were included for calculations of the spin distribution and for **A** matrices.

(15) Sheldrick, G. M. *Acta Crystallogr.*, *Sect. A* **1990**, *46*, 467.
(16) Sheldrick, G. M. *SHELXL 97. Program for the Refinement of Crystal Structures;* University of Göttingen; Göttingen, Germany, 1997.
(17) Frisch, M. J.; Trucks, G. W.; Schlegel, H. B.; Scuseria, G. E.; Robb, M. A.; Cheeseman, J. R.; Montgomery, J. A., Jr.; Vreven, T.; Kudin, K. N.; Burant, J. C.; Millam, J. M.; Iyengar, S. S.; Tomasi, J.; Barone, V.; Mennucci, B.; Cossi, M.; Scalmani, G.; Rega, N.; Petersson, G. A.; Nakatsuji, H.; Hada, M.; Ehara, M.; Toyota, K.; Fukuda, R.; Hasegawa, J.; Ishida, M.; Nakajima, T.; Honda, Y.; Kitao, O.; Nakai, H.; Klene, M.; Li, X.; Knox, J. E.; Hratchian, H. P.; Cross, J. B.; Bakken, V.; Adamo, C.; Jaramillo, J.; Gomperts, R.; Stratmann, R. E.; Yazyev, O.; Austin, A. J.; Cammi, R.; Pomelli, C.; Ochterski, J. W.; Ayala, P. Y.; Morokuma, K.; Voth, G. A.; Salvador, P.; Dannenberg, J. J.; Zakrzewski, V. G.; Dapprich, S.; Daniels, A. D.; Strain, M. C.; Farkas, O.; Malick, D. K.; Rabuck, A. D.; Raghavachari, K.; Foresman, J. B.; Ortiz, J. V.; Cui, Q.; Baboul, A. G.; Clifford, S.; Cioslowski, J.; Stefanov, B. B.; Liu, G.; Liashenko, A.; Piskorz, P.; Komaromi, I.; Martin, R. L.; Fox, D. J.; Keith, T.; Al-Laham, M. A.; Peng, C. Y.; Nanayakkara, A.; Challacombe, M.; Gill, P. M. W.; Johnson, B.; Chen, W.; Wong, M. W.; Gonzalez, C.; Pople, J. A. *Gaussian 03*, revision C.02; Gaussian, Inc.: Wallingford, CT, 2004.
(18) (a) te Velde, G.; Bickelhaupt, F. M.; van Gisbergen, S. J. A.; Fonseca Guerra, C.; Baerends, E. J.; Snijders, J. G.; Ziegler, T. *J. Comput. Chem.* **2001**, *22*, 931−967. (b) *ADF2005.01*; SCM, Theoretical Chemistry, Vrije Universiteit: Amsterdam, The Netherlands. http://www.scm.com.
(19) Becke, A. D. *J. Chem. Phys.* **1993**, *98*, 5648.
(20) Perdew, J. P.; Burke, K.; Ernzerhof, M. *Phys. Rev. Lett.* **1996**, *77*, 3865.
(21) (a) Hariharan P. C.; Pople, J. A. *Theor. Chim. Acta* **1973**, *28*, 213. (b) Rassolov, V. A.; Pople, J. A.; Ratner, M. A.; Windus, T. L. *J. Chem. Phys.* **1998**, *109*, 1223.
(22) Andrae, D.; Häussermann, U.; Dolg, M.; Stoll, H.; Preuss, H. *Theor. Chim. Acta* **1990**, *77*, 123.

Scheme 1
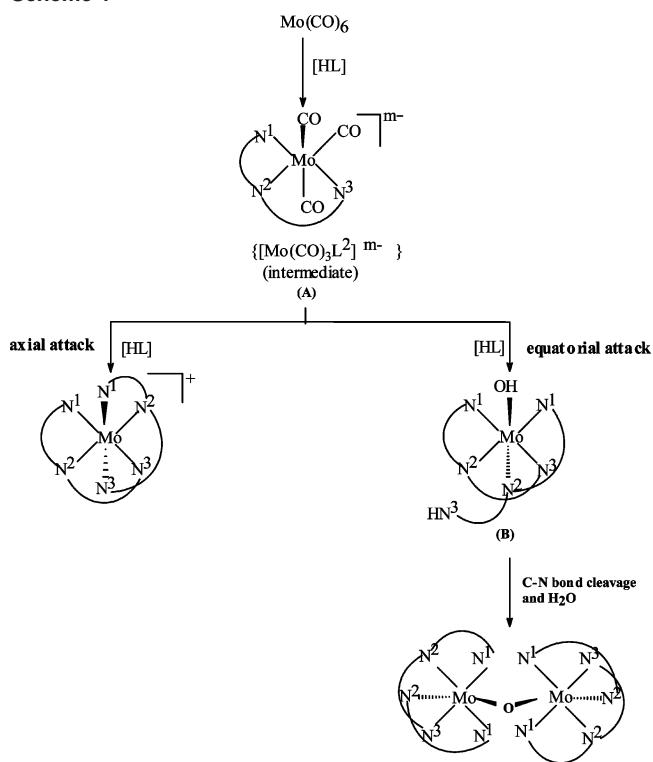
Within ADF, the functional including Becke's gradient correction to the local exchange expression in conjunction with Perdew's gradient correction to local density approximation with VWN parametrization of electron gas data was used (ADF/BP).[23]

Calculations were performed without any symmetry constraints. For radical anions, a spin-unrestricted Kohn−Sham formalism was used. For analysis of the singlet diradicals, a symmetry-breaking approach[24] within DFT is appropriate. Therefore, the calculations of the ground-state singlet states were performed using either spin-restricted or spin-unrestricted approaches (in G03, combined with GUESS=MIX). The lowest excited states were calculated using the time-dependent DFT method.

Results and Discussion

Synthesis. Two ligands, viz., HL^a and HL^b, differing with respect to substitution[9a] on the aminophenyl ring, are used in this work, and the isolated compounds are collected in Chart 1.

The ligands offer three very different kinds of N-coordination atoms, viz., a pyridyl-N (N^1), a reducible azo function containing N^2, and a diarylamido-N (N^3, after deprotonation). Pyridyl-N and azo-N are π-accepting, and reduced azo-N and diarylamido-N are π-donating. Crystallographic analysis shows meridional coordination (cf. Figure 3 below).

When reaction mixtures of Cr(CO)$_6$ and the ligands HL in 1:2 molar proportion were heated, brown compounds Cr-(L)$_2$ (**1a,b**) were isolated in ca. 70% yield. Similar reactions of Mo(CO)$_6$ yielded two brown compounds, **2** and **3**.

(23) (a) Becke, A. D. *Phys. Rev. A: At., Mol., Opt. Phys.* **1988**, *38*, 3098. (b) Perdew, J. P. *Phys. Rev. A: At., Mol., Opt. Phys.* **1986**, *33*, 8822.
(24) (a) Neese, F. *J. Phys. Chem. Solids* **2004**, *65*, 781. (b) Noodleman, L. *J. Chem. Phys.* **1981**, *74*, 5737. (c) Lahti, P. M.; Ichimura, A. S.; Sanborn, J. A. *J. Phys. Chem. A* **2001**, *105*, 251.

Compounds **2a,b**, isolated in ca. 65% yield, correspond to Mo(L)$_2$ as obtained[13] before from the reaction of (NH$_4$)$_6$-[Mo$_7$O$_{24}$]·4H$_2$O with HL in the presence of PPh$_3$. The minor products **3a,b**, are formed in ca. 5% yield; they are oxo-bridged dimolybdenum compounds with each metal ion coordinated by one tridentate ligand, one bidentate ligand pap, and a bridging oxide. The reactions of W(CO)$_6$ and HL, on the other hand, are sluggish and bis-chelated complexes W(L)$_2$ (**4a,b**) were obtained in ca. 45% yield after 120 h of reflux.

In the context of the formation of the two kinds of molybdenum complexes **2** and **3** from the same reaction, it appears that stepwise substitution[25,26] of CO together with the relative orientations of the coordinated ligands are key factors (Scheme 1). The partial substitution of three CO ligands from Mo(CO)$_6$ by one L$^-$ would produce a mixed-ligand intermediate [A]. This intermediate complex should have one equatorial and two axial CO ligands. An axial attack by the terminal pyridyl nitrogen of the second L$^-$ ligand would produce the bis-chelate **2**, whereas an equatorial attack would lead to the mixed ligand complex intermediate [B]. The source of [OH]$^-$ in this reaction could be moisture from the atmosphere or the solvent. Our proposition was further strengthened by the fact that the dimetallic complexes **3a** and **3b** do not form if the reaction is carried out in dry *n*-octane. Condensation and deamination of the intermediate [B] can produce the dinuclear complex **3**. The neutral hypodentate coordination mode of HL as in [B] was noted before, especially with 4d and 5d elements. Coordination of the pendant aryl amino function of the ligand is known[26,27] to effect C−N bond cleavage. No dimetallic compounds were isolated from the reactions of chromium and tungsten hexacarbonyls.

X-ray Crystal Structures. M(L)$_2$ (M = Cr (**1b**) and M = W (**4a**)). Single-crystal X-ray structure determination (Table 1) of the two representative chromium and tungsten complexes **1b** and **4a** revealed similar coordination and geometry to that of the molybdenum complex **2a**; they are considered together for comparison. The ORTEP representations with atom numbering schemes of **1b** and **4a** are depicted in Figures 1 and 2, respectively. The two deprotonated tridentate ligands are coordinated by the respective metal ion using pairs of pyridyl-N, azo-N, and deprotonated secondary amine (anilido) N atoms. The configuration is bis-meridional, and the relative orientations within the aforesaid pairs of coordinated atoms are cis, trans, and cis, respectively. Similar geometry and bonding was noted[13] before for the corresponding molybdenum complex **2a**. Notably, the average of the chelate bite angles, N(pyridyl)−M−N(azo) = 71.8° is systematically smaller than that of N(azo)−M−N(amide) = 76.5°, underlining the asymmetry of the mer-tridentate ligands.

The X-ray crystallographic analysis reveals considerably distorted-octahedral structures with trans-positioned azo-N, cis-positioned 2-pyridyl-N, and cis-oriented anilido nitrogen
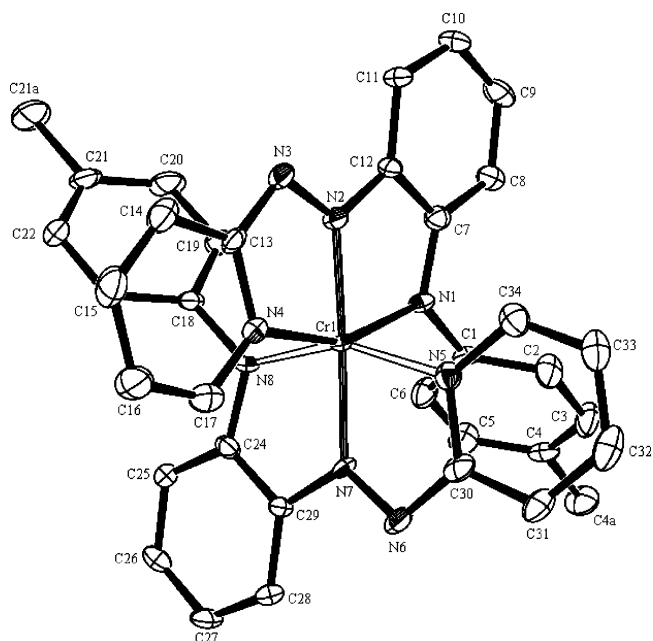

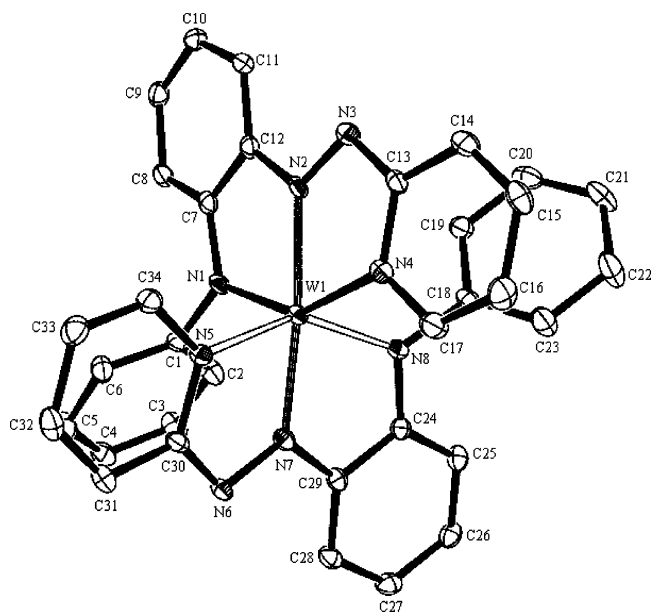**Figure 1.** ORTEP representation and atom numbering scheme for **1b**.

**Figure 2.** ORTEP representation and atom numbering scheme for **4a**.

atoms. The N$_{azo}$−M−N$_{azo}$ angle is larger than 170°; however, the other two trans angles are smaller at about 155° (M = Cr, **1b**) or 146° (M = Mo, W; **2a, 4a**) due to the overarching bite of the mer-tridentate ligands (Figure 3).

The bonds from M to the neutral 2-pyridyl-N atoms are distinctly longer (>0.08 Å) than those to the anilido or azo nitrogen atoms, reflecting negative charge on the latter.

The most notable part of the structures is the unusual elongation of the N−N bond lengths of the initial azo group. The averages of selected bond lengths are collected in Scheme 2, and Table 2 gives further details in connection with DFT calculation results.

(25) Jahng, Y.; Thummel, R. P.; Bott, S. G. *Inorg. Chem.* **1997**, *36*, 3133.

(26) Das, C.; Ghosh, A. K.; Hung, C.-H.; Peng, S.-M.; Lee, G.-H.; Goswami, S. *Inorg. Chem.* **2002**, *41*, 7125.

(27) Das, C.; Peng, S.-M.; Lee, G.-H.; Goswami, S. *New J. Chem.* **2002**, *26*, 222.
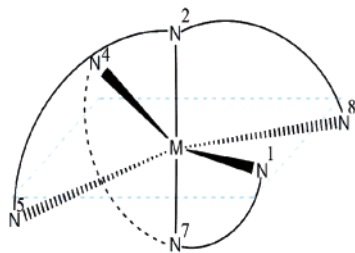
N^1, N^8 : N(anilido) N^2, N^7 : N(azo) N^4, N^5 : N(pyridyl)

Figure 3. Distorted-octahedral configuration of mononuclear complexes.

A view of the bond parameters of the three related complexes $M(L)_2$, M = Cr, Mo, W, reveals that the N−N bonds are considerably elongated relative to that in the uncoordinated protonated (2-pyridyl)-substituted ligand cation, $(H_2L')^+$ (Scheme 2), characterized[28] as $(H_2L')(ClO_4)$. Coordination of the ligand L^- to a metal ion is typically associated with the delocalization of the negative charge along the ligand backbone, resulting in a contraction of the C−N bonds on either side of the central *o*-phenylene ring and in an elongation of the azo bond. In the chromium complex **1b**, there have been contractions of the C−N bonds; however, the N−N bonds (av. 1.345(4) Å) are distinctly longer than the 1.308(3) Å observed in other examples[9] of $[M(L)_2]^{0/+}$ complexes (M = Co, Fe, Ni). On the other hand, the reference C−N bond lengths in the molybdenum and tungsten complexes **2a** and **4a** are similar to the single bond lengths observed in uncoordinated $(H_2L')^+$ (Scheme 2),[28] signifying the absence of electron delocalization. The average N−N bonds in these complexes **2a** and **4a** appear to become slightly longer than that in the chromium complex, all being comparable to the established[5a,7a,8a] N−N bond length of ca. 1.35 Å in metal-coordinated azo anion radical complexes. As a consequence of these structural results, the coordinated ligands have to be formulated as radical dianions, $L^{•2-}$, with one negative charge on the amide N and the other mainly located at the one-electron-reduced azo function. The metals would then be tetravalent in $[M^{IV}(L^{•2-})_2]$, implying a d^2 configuration. The metal−nitrogen bonds in these complexes are not unusual, the two M−N (py) bonds (to neutral N) being longer than the other four M−N bonds (which involve negatively charged N).

The molecular view and atom numbering scheme of the dimolybdenum compound **3a** are shown in Figure 4. Each molybdenum center is in a distorted-octahedral configuration: it is coordinated by one tridentate ligand $[L^a]^{•2-}$ and one apparently one-electron-reduced 2-(phenylazo)pyridine ligand, $pap^{•-}$, formed via the deamination of HL^a; the sixth position is occupied by a bridging oxide provided by moisture. In this example, there is considerable elongation of the azo bonds of *both* kinds of coordinated ligands, corresponding to a formulation $[Mo^{IV}_2(\mu\text{-}O^{2-})(pap^{•-})_2(L^{•2-})_2]$. Averages of selected bond distances are shown in Scheme 3. Little contraction of the C−N bonds on either side of the central

(28) Kamar, K. K.; Das, S.; Hung, C.-H.; Castiñeiras, A.; Kuźmin. M. D.; Rillo, C.; Bartolomé, J.; Goswami, S. *Inorg. Chem.* **2003**, *42*, 5367.

phenylene ring of the tridentate ligand is observed. Notably, in the structure of complex **2a**, the metal ion is in a distorted-octahedral environment consisting of two meridionally coordinated L^- ligands that have the azo nitrogen donors in a trans position. In contrast, the orientation of the two coordinated azo nitrogen donors in **3a** is cis.

The effects of N−N bond elongation of the coordinated ligands in the present complexes are reflected by the lowering of vibrational frequencies of $\nu_{N=N}$ as compared with that of uncoordinated HL. The $\nu_{N=N}$ band in free HL appears near 1380 cm^{-1} while those in the present complexes are considerably lower, between 1240 and 1280 cm^{-1}.
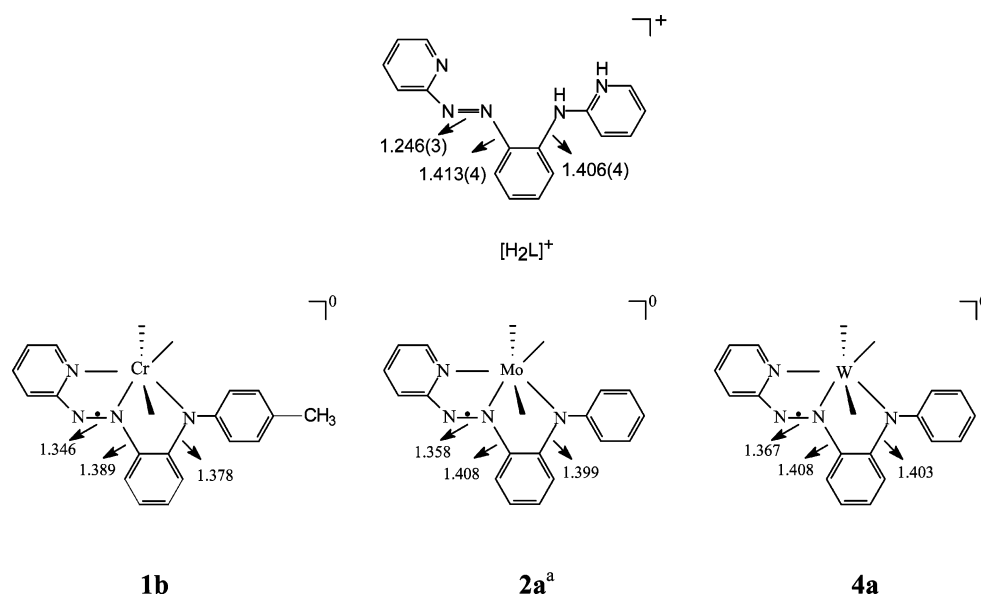
All complexes **1**−**4** possess $S = 0$ ground states as determined by magnetic susceptibility measurements at room temperature. They display sharp ^1H and ^{13}C NMR signals in the normal range for diamagnetic compounds. The NMR spectra reveal that the ligands in $M(L)_2$ are magnetically equivalent on the NMR time scale. The dimolybdenum complexes, on the other hand, show complex ^1H spectra due to the presence of several unique protons.

Diamagnetism in these complexes can arise from the pairing of electrons that are delocalized over the metal t_{2g} and ligand π^* orbitals or from strong antiferromagnetic coupling between unpaired spins of metal and ligand anion radicals. The ligand system under consideration exerts a strong field as evidenced by the previously reported low-spin $Mn^{II}(L)_2$ species[9b] with $S = {}^1/_2$. Moreover, the ligands are noninnocent and can undergo facile reduction on coordination with the electron addition occurring primarily at the azo function. This leads to alternative formulations I and II of the complexes according to Scheme 4.

The structural data for **2a** and **4a** indicate the absence of significant electron delocalization across the ligand backbone, specifically, the *o*-phenylene bridge. On the basis of the long N−N bonds present, we thus favor the $[M^{IV}(L^{•2-})_2]$ description (alternative II in Scheme 4). However, the X-ray diffraction data of the chromium complex **1b** suggest some degree of delocalization along the ligand backbone according to the resonance form in Scheme 5, indicating a reduced charge on the ligand but not enough to warrant a description according to alternative I of Scheme 4. The N−N bond lengths in other known complexes[9] of this ligand system did not exceed 1.308(3) Å whereas the average value in the present chromium complex is appreciably longer at 1.345-(4) Å. We thus conclude that, despite some degree of electron delocalization, the description $[Cr^{IV}(L^{•2-})_2]$ also contributes significantly to the electronic ground-state structure of this complex. The ligand π^* orbitals and the $d\pi$ orbitals of chromium are apparently closer, as confirmed by the DFT calculations. Finally, a comparison of the bond lengths in the dimetallic complex **3a** of molybdenum (Scheme 3) with those of monometallic **2a** leads to a corresponding formulation $[Mo_2^{IV}(\mu\text{-}O^{2-})(pap^{•-})_2(L^{•2-})_2]$.

The Electronic Structure of $[M(L)_2]^{0,-,+}$ (M = Cr, Mo, W). All neutral complexes examined are diamagnetic species; therefore, the geometry optimizations were done for singlet ground states. Calculations were done using both spin-restricted and spin-unrestricted approaches. The structures

Scheme 2 [a]

[H2L]+

1.246(3)
1.413(4)   1.406(4)

1.346
    1.389   1.378

1.358
    1.408   1.399

1.367
    1.408   1.403

1b   **2a**[a]   **4a**

[a] Ref 13.

Table 2. Selected Experimental and DFT (G03/PBE0) Calculated Symmetry-Averaged Bond Lengths (Å) and trans Angles (deg) of ML$_2$ Complexes
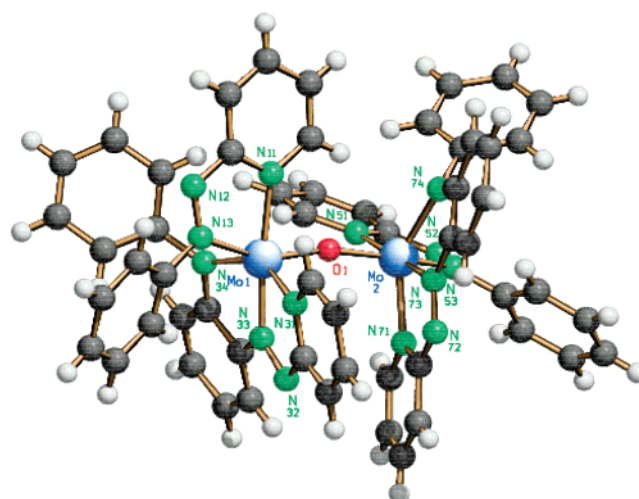
bond	M = Cr exp[a]	calcd[b]	M = Mo (2a) exp[c]	calcd	M = W (4a) exp	calcd
M−N1	1.940(2)	1.926	2.026(2)	2.029	1.997(2)	2.027
M−N8	1.927(2)		2.003(2)		2.014(2)	
M−N2	1.919(2)	1.896	2.025(2)	2.027	2.034(2)	2.039
M−N7	1.919(2)		2.038(2)		2.018(2)	
M−N4	2.028(2)	2.021	2.103(2)	2.114	2.095(3)	2.097
M−N5	2.029(2)		2.122(2)		2.079(2)	
N2−N3	1.353(2)	1.321	1.368(2)	1.338	1.361(3)	1.342
N6−N7	1.339(2)		1.347(2)		1.373(3)	
N2−C12	1.385(3)	1.379	1.398(3)	1.393	1.408(4)	1.400
N7−C29	1.393(3)		1.408(3)		1.408(4)	
N1−C7	1.375(3)		1.397(3)		1.406(4)	
N8−C24	1.381(2)		1.401(2)		1.399(4)	
N2−M−N7	170.17(7)		173.22(7)		172.45(9)	
N1−M−N4	155.46(7)		145.55(7)		146.98(10)	
N5−M−N8	155.57(7)		147.63(7)		145.05(10)	

[a] For **1b**. [b] For **1a**. [c] From ref 13.

Scheme 3

1.340(9)

1.387(11)

1.394(11)   1.348(10)

3a
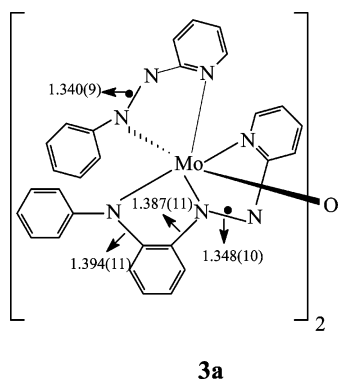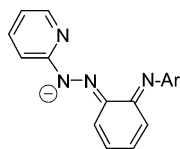
of all systems are better described by using the PBE0 hybrid functional than by using the B3LYP and depend only slightly on the approach used. Selected calculated bond lengths and angles are compared with the experimental ones in Table 2. The calculated structural parameters within all complexes are in very good agreement with experimental structures, and

Figure 4. Molecular view and atom numbering scheme for **3a**.

Scheme 4

M^{II}(L$^-$)$_2$
I

M^{IV}(L$^{•2-}$)$_2$
II

Ar = aryl

the variation of intraligand bond lengths is also well described by the calculations. The bond-length variation reflects the change of the central metal atom. The comparative calculations on the uncoordinated ligand (H$_2$L′)$^+$ and the analogous phenyl substituted ligand (HL) reproduced the N−N bond lengths within 0.01 Å, and the remaining bonding parameters are also well interpreted. Geometry optimization of the uncoordinated protonated (2-phenyl)-substituted ligand radical anion gave N−N, N2−C12, and N1−C7 bond lengths

Scheme 5

of 1.317, 1.365, and 1.397 Å, respectively. The elongation of the N−N bond due to the reduction of the ligand is comparable to the elongation caused by the specific metal coordination.

The comparison of DFT-calculated qualitative molecular orbital (MO) schemes for **1a**, **2a**, and **4a** is depicted in Figure 5, and the particular analysis of the virtual orbitals is listed in Tables S1−S3 (Supporting Information).

The MO representations are characterized by almost degenerate sets of highest occupied (HOMO) and lowest-lying unoccupied (LUMO) MOs formed by the combination of d metal orbitals and ligand orbitals. The HOMO of the chromium complex is to a large extent delocalized over the ligands; d orbitals contribute to this orbital by only 9%, and this d orbital is shifted to lower energy in the case of the Mo and W complexes. Two closely lying occupied MOs of **1a** have larger contributions (over 45%) from the central metal atom. The central metal atoms contribute to the LUMO from 41 to 57% when going from **1a** via **2a** to **4a**. The close-lying higher MOs have also relatively large contributions from the metal d orbitals, Figure 5 indicates their larger separation from the HOMO in the case of $Mo(L)_2$ and $W(L)_2$. The Mulliken population analysis indicates that the ligand L^- carries additional negative charge ranging from 0.66 (Cr complex) to 0.95 (W complex).

Cyclic Voltammetry, EPR, and UV−Vis−NIR Spectroelectrochemistry. Cyclic voltammetry of $Cr(L)_2$ (**1a,b**) in CH_2Cl_2 exhibits three reversible one-electron-transfer processes (two oxidations and one reduction; Table 3). The molybdenum and tungsten analogues show one reversible reduction. In addition, there are irreversible redox processes (Table 3). The dimolybdenum complexes **3a,b** display two successive one-electron reductions while the response on oxidation is not fully reversible (Figure 6).

The reversible redox processes were studied by EPR and UV−vis−NIR spectroelectrochemistry. Assuming a coupled $(L^{•2-})M^{IV}(L^{•2-})$ singlet diradical[29] ground state as suggested by structure and magnetism, the oxidation—reversible only for the chromium analogue—could lead to $[(L^-)M^{IV}(L^{•2-})]^+$, $[(L^-)M^{III}(L^-)]^+$, or to $[(L^{•2-})M^V(L^{•2-})]^+$ while the reduction should lead to $[(L^{•2-})M^{III}(L^{•2-})]^-$ since the ligands are
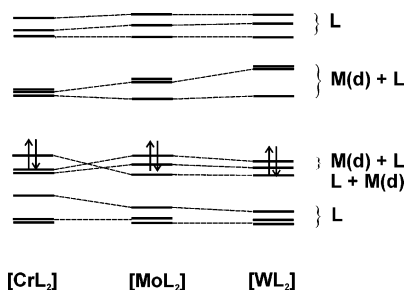

Figure 5. DFT-calculated qualitative MO scheme for $[ML_2]$.

Table 3. Cyclic Voltammetry Data[a]

compound	oxidation $E_{1/2}$,[b] V (ΔE_p, mV)	reduction $-E_{1/2}$,[b] V (ΔE_p, mV)
$[Cr(L^a)_2]$ (**1a**)	0.25(80), 1.10(70)	−0.48(80)
$[Cr(L^b)_2]$ (**1b**)	0.22(90), 1.02(80)	−0.52(80)
$[Mo(L^a)_2]$ (**2a**)	0.65[c]	−0.85(90), −1.80(90)
$[Mo(L^b)_2]$ (**2b**)	0.75[c]	−0.90(95), −1.85(90)
$[\{Mo(pap)(L^a)\}_2O]$ (**3a**)	0.35[c](200)	−1.05(90), −1.45(95)
$[\{Mo(pap)(L^b)\}_2O]$ (**3b**)	0.45[c](220)	−0.95(100), −1.25(80)
$[W(L^a)_2]$ (**4a**)	0.72[c]	−1.15(80)
$[W(L^b)_2]$ (**4b**)	0.75[c]	−1.17(95)

[a] In dichloromethane solution, with supporting electrolyte Bu_4NClO_4 (0.1 M) and a SCE reference electrode. [b] $E_{1/2} = 0.5(E_{pa} + E_{pc})$ where E_{pa} and E_{pc} are anodic and cathodic peak potentials respectively, and $\Delta E_p = E_{pa} - E_{pc}$; scan rate is 50 mV s^{-1}. [c] Irreversible.
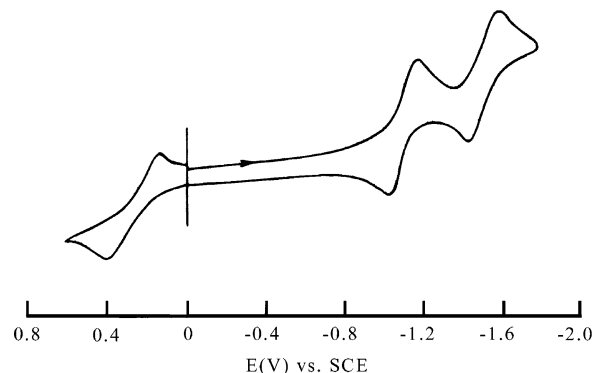

Figure 6. Cyclic voltammogram of **3a** in CH_2Cl_2/0.1 M Bu_4NClO_4.

unlikely to be reduced further. The diamagnetism of the starting complexes may be attributed to either strong anti-ferromagnetic coupling between the two radical dianion ligands alone, assuming a $S = 0$ state of the central tetravalent metal ("low-spin" d^2 configuration), or to a $S = 1$ configurated center ("high-spin" d^2) of which each electron couples with one of the radical ligands. The high-spin configuration would be more easily accessible for M = Cr whereas the heavier homologues should prefer the "low-spin" situation. Strong distortion from an ideal octahedral situation through the electronic asymmetry of the ligands and the structural distortion are expected to favor the low-spin arrangement.

Metal−ligand spin−spin coupling in the $[(L^-)Cr^{IV}(L^{•2-})]^+$ alternative (ligand oxidation) would produce metal-centered spin ($S = 1$ for Cr^{IV}, coupled with one $S = 1/2$ for one remaining radical); in the $S = 0$ situation of the metal, only one ligand-centered spin would remain. The other alternative, oxidation at the metal to $[(L^{•2-})M^V(L^{•2-})]^+$, is expected to create a three-spin situation with an *up, down, up* spin arrangement[30] because of the orthogonality of the mer-configurated radical dianion ligands. As a result, ligand-based spin would be expected.[30] For the chromium complex **1a**, the EPR experiment does not show a signal on oxidation,

(29) (a) Herebian, D.; Wieghardt, K.; Neese, F.; Weyhermüller, T. *J. Am. Chem. Soc.* **2003**, *125*, 10997. (b) Bill, E.; Bothe, E.; Chaudhuri, P.; Chlopek, K.; Herebian, D.; Kokatam, S.; Ray, K.; Weyhermüller, T.; Neese, F.; Wieghardt, K. *Chem.—Eur. J.* **2005**, *11*, 204.
(30) Ye, S.; Sarkar, B.; Lissner, F.; Schleid, Th.; van Slageren, J.; Fiedler, J.; Kaim, W. *Angew. Chem.* **2005**, *117*, 2140. Ye, S.; Sarkar, B.; Lissner, F.; Schleid, Th.; van Slageren, J.; Fiedler, J.; Kaim, W. *Angew. Chem., Int. Ed.* **2005**, *44*, 2103.
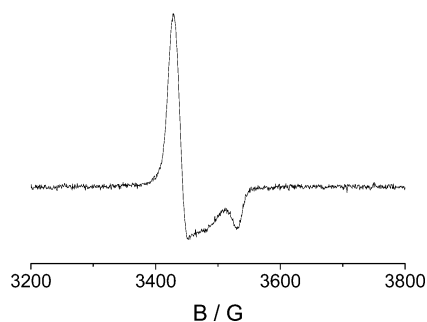
Figure 7. EPR spectrum of [Cr(L^a)$_2$]$^+$ (**1a$^+$**) at 110 K in CH$_2$Cl$_2$/0.1 M Bu$_4$NPF$_6$.
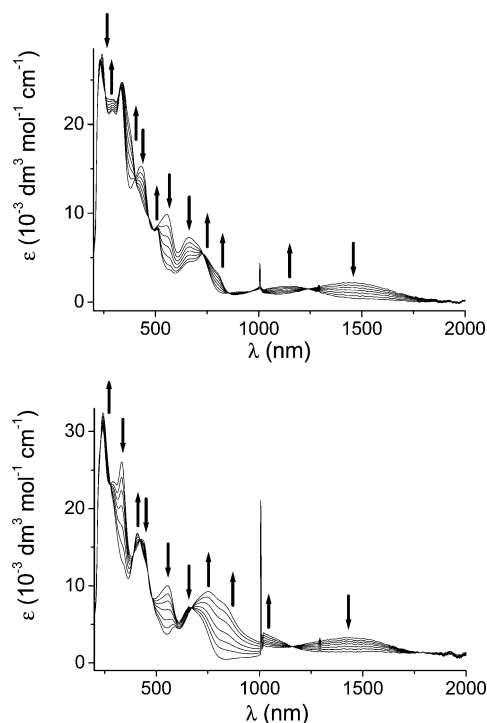
Figure 8. UV–vis–NIR spectroelectrochemistry for [Cr(L^a)$_2$] (**1a**) at 298 K in CH$_2$Cl$_2$/0.1 M Bu$_4$NPF$_6$; oxidation (top) and reduction (bottom).

even at 4 K. This result indicates very rapid relaxation and thus the presence of close-lying excited states, which would be more compatible with metal-centered spin in a [(L$^-$)M^{IV}-(L$^{•2-}$)]$^+$ situation (with $S_{Cr} = 1$) or with a [(L$^-$)M^{III}(L$^-$)]$^+$ description ($S_{Cr} = \frac{1}{2}$ or $\frac{3}{2}$). The DFT result with a predominantly metal-based HOMO (Table S1, Supporting Information) is in agreement with these results. The irreversibility of the oxidation of molybdenum or tungsten analogues may reflect the reluctance of these heavier elements to adopt the odd-electron M^{III} oxidation state.

One-electron reduction of **1a** yields an EPR signal showing metal-centered spin with $g_{\parallel} = 1.954$ and $g_{\perp} = 2.005$ (Figure 7). The [(L$^{•2-}$)M^{III}(L$^{•2-}$)]$^-$ oxidation-state combination would lead to such a result in the case of high-spin Cr^{III} ($S = \frac{3}{2}$) through two antiferromagnetic coupling interactions of radical spin/metal spin, leaving one remaining unpaired electron at chromium(III).[31]

The molybdenum and tungsten analogues exhibit weak EPR signals around $g = 2$ on one-electron reduction,

Table 4. UV–Vis–NIR Data^a from Spectroelectrochemistry in CH$_3$CN/0.1 M Bu$_4$NPF$_6$

compound	$\lambda_{max}{}^a$ (ϵ)
1a	1445(2200), 727sh, 663(7300), 555(9900), 431(15400), 333(24000), 290sh, 241(28000)
1a$^-$	1148(1800), 805sh, 730(5400), 658sh, 508(8200), 427sh, 383sh, 340(24700), 294sh, 230(27300)
1a$^+$	1030sh, 833sh, 754(9300), 675(sh), 450sh, 408(16800), 295(sh), 242(32400)
1a^{2+}	915(3900), 809(5400), 564(8900), 475sh, 383(18800), 242(28300)
2a	680(2500), 460(18100), 388(20600), 303(31800), 266sh, 241sh
2a$^-$	585sh, 465(18200), 365sh, 303(32800), 265sh, 240sh
3a	485(9700), 370(13200), 295(23100), 275sh, 236(21500)
3a$^-$	457sh, 369sh, 296(22900), 239(24200)
3a$^+$	731(2800), 475(10100), 373sh, 288(18400), 236(21700)
4a	578(2800), 420sh, 373(17900), 300(24900), 267(24300), 242sh
4a$^-$	410(13900), 345(19300), 301(25300), 268(24900), 240sh

^{a} Wavelengths in nm and molar extinction coefficients in M^{-1} cm^{-1}.

reflecting low-spin M^{III} ($S = \frac{1}{2}$) coupled antiferromagnetically with two radicals in an up, down, up spin arrangement[30] with largely ligand-centered spin. DFT results have not been conclusive with regard to the reduction since the LUMO was calculated to be metal–ligand mixed in all instances.

The chromium complex **1a** shows clean spectroelectrochemical behavior for one reduction and two oxidation steps; however, the large number of bands in the UV, vis, and NIR regions (Figure 8 and Table 4) makes a definite assignment difficult.

The near-IR band at 1445 nm for the neutral form, possibly involving [(L$^{•2-}$)Cr^{III}(L$^-$)]* as the excited state in a ligand-to-metal charge transfer (LMCT) transition, disappears on oxidation to [(L$^-$)Cr^{IV}(L$^{•2-}$)]$^+$ while a new band system emerges at around 800 nm. On second oxidation, this band system is diminished whereas absorption intensity is gained in the high-energy part of the visible spectrum. On reduction to [(L$^{•2-}$)Cr^{III}(L$^{•2-}$)]$^-$ of **1a$^-$**, the near-IR band is apparently shifted to higher energies at 1148 nm, suggesting an LMCT process.

The reversible reduction of the molybdenum and tungsten compounds produces little spectral change (Figure S2, Supporting Information).

At 4 K, the dinuclear compound **3a** shows narrow but unresolved EPR signals at $g = 2.00$ for both the oxidized and reduced forms. Such a weak signal is also observed qjfor the native state. Since the compound contains the L$^{•2-}$ and pap$^{•-}$ radical ions as ligands on either side of the molecule, any one-electron process would remove the spin–spin coupling balance to produce a radical-type EPR signal. As for the mononuclear species **2a**, the spectroelectrochemistry does not show extensive change on reduction or oxidation.

Conclusion

Herein, we have reported a general synthesis of diamagnetic complexes of group VI metal ions with azo dianion

(31) Goodman, B. A.; Raynor, J. B. *Adv. Inorg. Chem. Radiochem.* **1970**, *13*, 135.

radical ligands from the corresponding metal carbonyls. The synthesis of the molybdenum complexes (**2a,b**) was achieved before from ammonium heptamolybdate using PPh$_3$ as the reducing agent; however, other polyoxometalates such as (NH$_4$)$_2$[CrO$_4$] or (NH$_4$)$_{10}$[W$_{12}$O$_{41}$]·5H$_2$O have failed to react under the same experimental conditions. X-ray structural data of the mononuclear complexes ML$_2$ (M = Cr, Mo, W) indicate that two meridionally coordinated ligand dianion radicals bind to a tetravalent (M^{IV}) metal ion, as evident from the characteristic bond elongation within the azo chromophores. Bond−structure parameters supported by magnetic, redox, and spectroscopic data and by DFT calculations suggest a singlet diradical description of the mononuclear [M^{IV}(L$^{•2-}$)$_2$] complexes wherein the two ligand π radicals are intramolecularly antiferromagnetically coupled, affording a diamagnetic ($S = 0$) ground state in each case. Finally, we also have reported unusual dimolybdenum complexes from the above reaction. The dinuclear compounds possess a diamagnetic ground state, and their electronic structures are best described as consisting of two [Mo^{IV}(L$^{•2-}$)(pap$^{•-}$)] units bridged via O^{2-}: [Mo^{IV}(L$^{•2-}$)(pap$^{•-}$)]$_2$O.

Supporting Information Available: X-ray crystallographic files in CIF format for **1b**, **3a** and **4a**; figures of virtual orbitals for WL$_2$ (S1), cyclic voltammogram of **1b** (S2), and UV−vis−NIR spectroelectrochemistry (reduction) for **2a** at 298 K in CH$_2$Cl$_2$/0.1 M Bu$_4$NPF$_6$ (S3). This material is available free of charge via the Internet at http://pubs.acs.org.

IC700584X